Behavioral/Cognitive

NR2A-Containing NMDARs in the Prefrontal Cortex Are Required for Working Memory and Associated with Age-Related Cognitive Decline

Joseph A. McQuail,[1] B. Sofia Beas,[1] Kyle B. Kelly,[2] Kailey L. Simpson,[1] Charles J. Frazier,[2,4] Barry Setlow,[1,3,4] and Jennifer L. Bizon[1,3,4]

[1]Department of Neuroscience, College of Medicine, [2]Department of Pharmacodynamics, College of Pharmacy, [3]Department of Psychiatry, College of Medicine, and [4]McKnight Brain Institute, University of Florida, Gainesville, Florida 32610

Working memory, the ability to temporarily maintain representational knowledge, is a foundational cognitive process that can become compromised in aging and neuropsychiatric disease. NMDA receptor (NMDAR) activation in prefrontal cortex (PFC) is necessary for the pyramidal neuron activity believed to enable working memory; however, the distinct biophysical properties and localization of NMDARs containing NR2A and NR2B subunits suggest unique roles for NMDAR subtypes in PFC neural activity and working memory. Experiments herein show that working memory depends on NR2A- but not NR2B-NMDARs in PFC of rats and that NR2A-NMDARs mediate the majority of evoked NMDAR currents on layer 2/3 PFC pyramidal neurons. Moreover, attenuated expression of the NR2A but not the NR2B subunit in PFC associates with naturally occurring working memory impairment in aged rats. Finally, NMDAR currents and working memory are enhanced in aged rats by promoting activation of the NR2A-enriched synaptic pool of PFC NMDARs. These results implicate NR2A-NMDARs in normal working memory and suggest novel treatment strategies for improving working memory in cognitive disorders.

Key words: **aging; cognition; NMDA receptor; prefrontal cortex; rat; working memory**

Significance Statement

Working memory, the ability to hold information "in mind," requires persistent activity of pyramidal neurons in prefrontal cortex (PFC) mediated by NMDA receptor (NMDAR) activation. NMDAR loss in PFC may account for working memory impairments in aging and psychiatric disease. Our studies demonstrate that NMDARs containing the NR2A subunit, but not the NR2B subunit, are required for working memory and that loss of NR2A predicts severity of age-related working memory impairment. The importance of NR2A to working memory is likely due its abundant contribution to pyramidal neuron activity and location at synaptic sites in PFC. This information is useful in designing new therapies to treat working memory impairments by enhancing the function of NR2A-containing NMDARs.

Introduction

Working memory is a flexible form of short-term memory used to guide ongoing, goal-directed behavior (Baddeley, 1986). Working memory is supported by the prefrontal cortex (PFC) and is believed to rely on the ability of pyramidal neuron networks to persist in firing even after a to-be-remembered stimulus is removed from the environment (Goldman-Rakic, 1995). Ionotropic glutamate receptors of the NMDA subtype (NMDARs) are expressed on PFC pyramidal neurons and altered activity at these receptors has been implicated in working memory deficits associated with both psychiatric disorders and normal aging. Indeed, blockade of NMDARs interferes with persistent activity of pyramidal neurons after the presentation of a sensory stimulus (Wang et al., 2013) and systemic administration of NMDAR antagonists reliably impairs performance on behavioral tasks that are used across species to evaluate working memory (Smith et al., 2011; Wang et al., 2013).

NMDARs are tetramers comprised of two obligatory NR1 and two regulatory NR2A or NR2B subunits. Expression of the NR2 subunit is developmentally regulated. Specifically, NR2B subunits commonly expressed in the immature brain are progres-

Received July 19, 2016; revised Oct. 24, 2016; accepted Oct. 24, 2016.

Author contributions: J.A.M., B.S.B., C.J.F., B.S., and J.L.B. designed research; J.A.M., B.S.B., K.B.K., K.L.S., and C.J.F. performed research; J.A.M., B.S.B., K.B.K., C.J.F., and J.L.B. analyzed data; J.A.M., C.J.F., B.S., and J.L.B. wrote the paper.

This work was supported by the National Institutes of Health (Grant AG051371 to J.A.M. and Grant AG029421 to J.L.B.), the National Science Foundation (Graduate Research Fellowship Program Grant DGE-0802270 to B.S.B.), and the McKnight Brain Research Foundation (J.L.B.). We thank Cristina Bañuelos, Caesar Hernandez, Vicky Kelley, Bonnie McLaurin, Miranda Schwabe, Lauren Vetere, and Shannon Wall for technical assistance.

The authors declare no competing financial interests.

Correspondence should be addressed to Jennifer L. Bizon, Ph.D., Department of Neuroscience, McKnight Brain Institute, University of Florida, P.O. Box 100244, Gainesville, FL 32610. E-mail: bizonj@ufl.edu.

DOI:10.1523/JNEUROSCI.2332-16.2016

 0270-6474/16/3612537-12$15.00/0

sively replaced by NR2A subunits that become dominant in adult brain (Sheng et al., 1994; Sans et al., 2000). These changes in NR2 subunits across the lifespan have significant consequences for neural transmission because NR2A- and NR2B-containing NMDARs differ with respect to biophysical properties (Vicini et al., 1998; Erreger et al., 2005; Hansen et al., 2014), synaptic localization (Townsend et al., 2003; Groc et al., 2006), activity-dependent trafficking (Barria and Malinow, 2002), and contributions to synaptic plasticity (Liu et al., 2004; Massey et al., 2004). Unique characteristics conferred by each NR2 subunit favor a preferred role in working memory. For example, the slower decay kinetics of the NR2B subunit relative to NR2A (Vicini et al., 1998; Erreger et al., 2005; Hansen et al., 2014) could facilitate the summation of excitatory inputs necessary for persistent firing after sensory stimulation (Wang et al., 2008, 2013). Conversely, NR2A-NMDARs are most commonly anchored at the synapse (Tovar and Westbrook, 1999; Townsend et al., 2003; Groc et al., 2006), where they are well positioned to support activity-dependent signaling, including recurrent excitation that enables working memory. Defining the respective contributions of NR2A- and NR2B-NMDARs to working memory could inform new therapeutic approaches to treat cognitive disorders; however, no studies to date have directly evaluated working memory after blockade of individual NMDAR subtypes within the PFC.

Across species, working memory impairment is a hallmark of the normal aging process (Oscar-Berman and Bonner, 1985; Dunnett et al., 1988; Rapp and Amaral, 1989; Bachevalier et al., 1991; Lamar and Resnick, 2004; Beas et al., 2013). Although most extensively studied within the context of the hippocampus and long-term memory (Burke and Barnes, 2010; Foster, 2012), reduced NMDAR expression and activity are also observed in the aged PFC (Magnusson, 2000; Magnusson et al., 2002; Zhao et al., 2009; Zamzow et al., 2013; Guidi et al., 2015). It is unknown, however, the extent to which altered NMDAR expression in aged PFC contributes to working memory decline and if modulating NMDARs in the aged PFC can improve cognition in older subjects.

The goals of this study were threefold. First, we tested the effects of acute pharmacological blockade of distinct PFC NMDAR subtypes on working memory performance in young rats. Second, we determined the degree to which attenuated expression of NMDAR subunits associates with working memory decline among aged rats. Third, we determined whether acute positive modulation of PFC NMDARs in aged rats is sufficient to improve working memory performance. Broadly, our findings implicate the NR2A subunit in normal working memory function and reduced PFC expression of the NR2A subunit in the decline of working memory that accompanies the aging process. These findings suggest targeting of NR2A-NMDARs as a novel therapeutic strategy for treating cognitive decline at advanced ages.

Materials and Methods

Subjects

Male young adult (4–6 months old, $n = 58$) and aged (22–26 months old, $n = 30$) Fischer 344 rats were acquired from the National Institute on Aging Rodent Colony (housed at Charles River Laboratories). In Experiment 1, $n = 40$ young rats were used for behavioral pharmacological experiments that assessed working memory performance after blockade of medial PFC (mPFC) NR2A or NR2B receptors, $n = 7$ young rats were used for patch-clamp electrophysiology experiments that evaluated the relative contributions of NR2A and NR2B receptors to the overall NMDAR-mediated evoked EPSC in mPFC pyramidal neurons, and $n = 3$ young rats were used for coimmunoprecipitation experiments to determine NR2A–PSD95 associations in mPFC. In Experiment 2, $n = 8$ young and $n = 13$ aged rats were used to evaluate age-related changes in mPFC expression of excitatory signaling proteins and their relationship with individual differences in working memory ability. In Experiment 3, $n = 11$ aged rats were used to test the effects of modulation of NMDAR activity on working memory performance and $n = 6$ aged rats were used for patch-clamp electrophysiology experiments to evaluate the effects of a D-amino acid oxidase inhibitor on evoked NR2A-NMDAR currents. Across experiments, rats were housed individually with *ad libitum* access to food and water except during behavioral testing as described below. All animal procedures were approved by the Institutional Animal Care and Use Committee of the University of Florida and conformed to the National Institutes of Health's animal welfare guidelines.

Experiment 1: Determining the role of NMDAR subtypes in working memory and mPFC neural physiology

Surgical procedures. Rats were anesthetized with isofluorane gas and fixed into a stereotaxic frame (Kopf Instruments) fitted with atraumatic ear bars. The incisor bar was set at −3.3 mm relative to the interaural line to provide a flat skull position. A midline incision was made and the skin and fascia over the skull were retracted. Burr holes were drilled in the skull over the mPFC for placement of three stainless steel screws. Bilateral guide cannulae, consisting of a plastic body holding two 22-gauge stainless steel cannulae spaced 1.4 mm apart (Plastics One) were implanted to target mPFC at the coordinates (in mm) AP: +2.7 from bregma, ML: ±0.7 from bregma, DV: −3.8 from the skull surface. Cannulae were secured to the skull with stainless steel screws and dental acrylic and wire stylets were placed in the guide cannulae to prevent infection. Rats received injections of buprenorphine (1 mg/kg/d for 2 d postoperatively) and meloxicam (2 mg/kg/d for 3 d postoperatively) and topical triple antibiotic ointment (as needed) for analgesia and to prevent infection. Rats were given a 2 week recovery period before beginning behavioral testing.

Behavioral testing apparatus. Testing in the delayed response task (DRT) used to assess working memory was conducted in eight identical standard rat behavioral test chambers (30.5 × 25.4 × 30.5 cm; Coulbourn Instruments) with metal front and back walls, transparent Plexiglas side walls, and a floor composed of steel rods (0.4 cm diameter) spaced 1.1 cm apart. Each test chamber was housed in a sound-attenuating cubicle and was equipped with a recessed food pellet delivery trough located 2 cm above the floor in the center of the front wall. The trough was fitted with a photobeam to detect head entries and a 1.12 W lamp for illumination. A single 45 mg grain-based food pellet (5TUM; TestDiet) was delivered to reward correct responses. Two retractable levers were located to the left and right of the food trough (11 cm above the floor). An additional 1.12 W house light was mounted near the top of the rear wall of the sound attenuating cubicle. Behavioral test chambers were connected to a computer running Graphic State 3.01 software (Coulbourn Instruments) that controlled experiments and recorded responses.

Habituation and initial shaping of operant procedures. Before the start of behavioral testing, rats were reduced to 85% of their free-feeding weights over the course of 5 d and maintained at these weights for the duration of behavioral testing. Rats progressed through three stages of shaping before the start of the DRT, with a new stage beginning on the day immediately after completion of the previous stage. On the day before Shaping Stage 1, each rat was given five 45 mg food pellets in its home cage to reduce neophobia to the food reward used in the task. Shaping Stage 1 consisted of a 64 min session of magazine training, involving 38 deliveries of a single food pellet with an intertrial interval of 100 ± 40 s. Shaping Stage 2 consisted of lever press training, in which a single lever (left or right, counterbalanced across animals) was extended and a press resulted in delivery of a single food pellet. After reaching a criterion of 50 lever presses in 30 min, rats were then trained on the opposite lever using the same procedures. During Shaping Stage 3, the left or right lever (counterbalanced across trials in this stage of testing) was extended into the chamber and each press resulted in a single food pellet delivery. Rats

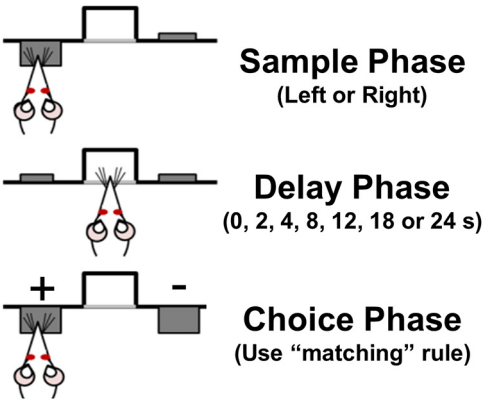

Figure 1. Schematic of the DRT of working memory. The DRT includes three phases in each trial. In the sample phase, one lever (either left or right, pseudorandomly varied between trials) is extended into the chamber. Once the rat presses the lever, it is retracted and a delay phase is initiated (pseudorandomly varied from 0 to 24 s) in which the rat must continuously nose poke in the centrally located food trough. After the delay period, the choice phase involves the extension of both levers (left and right) into the chamber. The rat must remember the lever presented during the sample phase and choose that lever to receive a food reward (+ = positively reinforced/correct choice; − = nonreinforced/incorrect choice).

were trained in Shaping Stage 3 until achieving 80 lever presses in a 30 min session.

DRT behavioral procedures. The DRT (Fig. 1) is modeled after that described by Sloan et al. (2006)) and has been used in our laboratory previously to demonstrate age-related working memory impairments in Fischer 344 rats (Beas et al., 2013; Bañuelos et al., 2014; McQuail et al., 2015). The duration of each session was 40 min and the house light was illuminated throughout the entire session except during timeout periods (see below). Rats received one test session per day. The extension of a single lever (the "sample" lever) into the chamber served to initiate a trial, with the left/right position of the sample lever randomized within each pair of trials. A lever press caused the sample lever to retract and initiated the delay period timer. Rats were required to nose poke into the central food trough during the delay interval. The first nose poke after expiration of the delay interval initiated the "choice" phase of the task in which both levers extended into the chamber. If the rat pressed the same lever as that pressed during the sample phase (a correct response), both levers were retracted and a single food pellet was delivered. Entry into the food trough to collect the food pellet initiated a 5 s intertrial interval, after which the next trial was initiated. If the rat pressed the opposite lever from that chosen during the sample phase (an incorrect response), both levers were retracted and the rat received a 5 s "timeout" period during which the house light was extinguished. The next trial began immediately upon conclusion of the timeout period. During initial sessions in this task, there were no delays between the sample and choice phases and a correction procedure was used such that the sample lever was repeated on the same side after an incorrect response to prevent development of side biases. Once rats reached a criterion of 80% correct choices across a session for two consecutive sessions, this correction procedure was discontinued and a set of seven delays was introduced. The presentation of delay durations was randomized within each block of seven trials such that each delay was presented once per block. Upon establishing >80% correct performance across two consecutive sessions at a set of delays, rats were progressed to the next set: Set 1: 0, 1, 2, 3, 4, 5, 6 s; Set 2: 0, 2, 4, 8, 12, 16 s; and Set 3 ("final set"): 0, 2, 4, 8, 12, 18, and 24 s. Before drug microinjections, rats were trained on the final set of delays for at least 1 week (during which they were required to complete at least 65 trials per session).

Drug preparation and administration. NVP-AAM077 tetrasodium hydrate (NVP; PEAQX or [(1S)-1-(4-bromophenyl)ethyl]amino](1,2,3,4-tetrahydro-2,3-dioxo-5-quinoxalinyl)methyl] phosphonic acid tetrasodium hydrate), a competitive NR2A-preferring antagonist (Auberson et al., 2002; Frizelle et al., 2006; Neyton and Paoletti, 2006), was obtained from Sigma-Aldrich (catalog #P1999). NVP was dissolved in 10% DMSO (Fisher Scientific) in artificial CSF (aCSF; Harvard Apparatus) to concentrations of 0.3, 1, or 3 μg per 0.5 μl. These doses were based on prior studies showing that intracerebral microinjection of NVP impairs fear learning (Walker and Davis, 2008; Zhang et al., 2008). TCN-201 (TCN;3-chloro-4-fluoro-*N*-[4-[[2-(phenylcarbonyl)hydrazino]carbonyl]benzyl]benzenesulfonamide), a noncompetitive NR2A-selective antagonist (Bettini et al., 2010; Edman et al., 2012; Hansen et al., 2012), was purchased from Tocris Bioscience (catalog #4154). TCN was initially dissolved in pure DMSO and diluted with aCSF to concentrations of 0.23, 2.3, and 23 fg per 0.5 μl; the final concentration of DMSO was 0.1% (v/v). These doses were selected based on a previous report (Gipson et al., 2013) showing that 2.3 and 23 fg of TCN microinjected into the nucleus accumbens reduces cue-induced nicotine seeking. Ro 25–6981 maleate (Ro 25; (αR,βS)-α-(4-hydroxyphenyl)-β-methyl-4-(phenylmethyl)-1-piperidinepropanol maleate), a noncompetitive NR2B-selective antagonist (Fischer et al., 1997), was purchased from Tocris Bioscience (catalog #1594) and dissolved in aCSF at final concentrations of 2, 6, and 18 μg per 0.5 μl. These doses were based on prior studies showing that 2.5 μg of Ro 25 microinjected into the rodent mPFC impairs odor span memory and reversal learning (Brigman et al., 2013; Davies et al., 2013). Ifenprodil hemitartrate ((1R*,2S*)-erythro-2-(4-benzylpiperidino)-1-(4-hydroxyphenyl)-1-propanol hemitartrate), also a noncompetitive NR2B-selective antagonist (Gallagher et al., 1996; Fischer et al., 1997), was purchased from Tocris Bioscience (catalog #545). Ifenprodil was dissolved in 2% (w/v) (2-hydroxypropyl)-β-cyclodextrin (Sigma-Aldrich) in aCSF and diluted to final concentrations of 1.2, 4, and 12 μg per 0.5 μl. These doses were selected based on previous studies showing that intra-mPFC microinjection of 2 μg of ifenprodil blocks fear conditioning and extinction (Laurent and Westbrook, 2008; Sotres-Bayon et al., 2009).

Within each cohort of rats (NVP: $n = 9$; TCN: $n = 11$; Ro 25: $n = 11$; ifenprodil: $n = 9$), doses were administered using a randomized, within-subjects design such that each rat received each dose of the drug and vehicle, with a 48 h washout period between successive doses. Drugs were administered 10 min before the start of behavioral testing each day using 10 μl syringes mounted on a syringe pump (Pump 11 Elite; Harvard Apparatus) and connected to injection needles by a length of PE-20 tubing. For microinjections, rats were gently restrained by hand, the stylets removed from the guide cannulae, and bilateral microinjection needles (Plastics One) that extended 1 mm beyond the guide cannulae were inserted. Drugs were administered in a volume of 0.5 μl/hemisphere delivered over 1 min and injection needles were left in place for an additional minute after the injection to allow for drug diffusion.

Histological verification of cannula placements. After completion of behavioral testing, rats were administered a lethal injection of Euthasol (sodium pentobarbital and phenytoin solution; Virbac) and then perfused with 0.1 M PBS followed by 4% paraformaldehyde in 0.1 M PBS (all chemicals purchased from Fisher Scientific). Brains were removed and postfixed in 4% paraformaldehyde overnight and cryoprotected in 20% sucrose in PBS. Brains were then flash frozen and sliced coronally at 50 μm on a cryostat (Leica Jung Frigocut 2800E). Every second section was mounted on charged glass slides and stained with thionin. Cannula tip placements were visualized using a microscope under conventional bright-field illumination and mapped onto standardized coronal sections of the rat brain (Paxinos and Watson, 2005). Only those rats with placements found to terminate within the boundaries of the prelimbic or infralimbic cortex were included in the behavioral analysis. The placements of cannulae for each cohort are shown in Figures 2 and 3.

Electrophysiology methods. Whole-cell patch-clamp experiments were performed to isolate the individual contributions of NR2A- and NR2B-containing NMDARs to the overall NMDAR-mediated evoked EPSC (Massey et al., 2004; Liu et al., 2004; eEPSC). All chemicals used for electrophysiology were obtained from Tocris Bioscience, Sigma-Aldrich, or Fisher Scientific. Young adult rats ($n = 7$) were anesthetized with an intraperitoneal injection of 100 mg/kg ketamine and 10 mg/kg xylazine and then perfused transcardially with sucrose-laden aCSF containing the following (in mM): 206 sucrose, 2 KCl, 25 $NaHCO_3$, 1.2 NaH_2PO_4, 1 $CaCl_2$, 1 $MgSO_4$, 0.01 glycine, and 10 D-glucose saturated with 95% O_2 and 5% CO_2. After perfusion, animals were decapitated, the brains extracted, and 300-μm-thick coronal slices were made through the mPFC in ice-cold aCSF using a Leica VT1000s vibratome. Slices were trans-

ferred to an incubator containing sucrose-free aCSF containing the following (in mM): 124 NaCl, 2.5 KCl, 25 $NaHCO_3$, 1.23 NaH_2PO_4, 1 $CaCl_2$, 3 $MgSO_4$, and 10 D-glucose saturated with 95% O_2 and 5% CO_2 that was preheated to 30–35°C for 30 min and then equilibrated to room temperature for a least 60 min before experimental use. After incubation, slices were transferred to a recording chamber where they were perfused at 2 ml/min with magnesium-free aCSF containing the following (in mM): 129 NaCl, 3 KCl, 25 $NaHCO_3$, 1.2 NaH_2PO_4, 2.4 $CaCl_2$, and 11 D-glucose saturated with 95% O_2 and 5% CO_2 and temperature was maintained at 30 ± 2°C. To record evoked EPSCs (eEPSCs), the patch electrode internal solution contained the following (in mM): 130 K-Glu, 10 KCl, 5 NaCl, 2 $MgCl_2$, 0.1 EGTA, 2 Na_2-ATP, 0.3 Na-GTP, 10 HEPES, and 10 phosphocreatine and electrode tip resistance was 3–5 MΩ. In addition, a 1 mM concentration of the chloride channel blocker 4,4′-dinitrostilbene-2,2′-disulfonic acid (DNDS) was added to the internal solution; this eliminated the $GABA_A$ activity of the patched cell while leaving the GABA signaling of the rest of the slice intact, thus avoiding epileptiform activity. Cells selected for patching were visualized with infrared differential interference contrast microscopy using an Olympus BX51WI microscope. Access resistance, membrane resistance, and whole-cell capacitance were measured in voltage-clamp mode in response to a −10 mV hyperpolarizing step delivered every 10 s. Cells were discarded if access resistance changed by ~30% or more during the course of an experiment. To generate eEPSCs, a theta tip glass electrode filled with extracellular solution was connected to a constant current stimulus isolator (World Precision Instruments) and placed in layer 2/3 (L2/3). Stimuli lasting 0.1 ms were delivered at a frequency of 0.1 Hz. Voltage-clamp recordings were performed using an Axon Multiclamp 700B amplifier (Molecular Devices). Data were sampled at 20 kHz, filtered at 2 kHz, and digitally recorded by a Digidata 1440 A/D converter using Clampex version 10 (Molecular Devices). Bath application of 10 μM NBQX was maintained throughout the experiment to block AMPAR-mediated currents. After a 5 min stable baseline, the NMDAR-mediated current was blocked by the sequential addition of 1 μM Ro 25–6981 (Tocris Bioscience, catalog #1594), followed 10 min later by 0.4 μM NVP-AAM077 (Sigma-Aldrich, catalog #P1999).

Tissue preparation, coimmunoprecipitation, and Western blotting of PSD-95-bound proteins. The mPFC was dissected from previously frozen brain tissue ($n = 3$ young adult rats; 4–6 months). The frontal cortex was sectioned at a nominal thickness of 360 μm and tissue punches from the mPFC were made using a 1 mm biopsy punch and stored at −80°C. Tissue punches were pooled, weighed, and then homogenized in 10 volumes of ice-cold buffer (320 mM sucrose and 1 mM EDTA in 10 mM Tris, pH 7.4) supplemented with Halt protease inhibitors (Fisher Scientific). The homogenate was centrifuged at 1000 × *g* for 10 min at 4°C. The supernatant was transferred to a fresh tube and lysed by the addition of 0.1 volume of 10% (w/v) sodium deoxycholate in 500 mM Tris, pH 9.0, with agitation at 37°C for 45 min. After adding 0.1 volume of 10 × immunoprecipitation (IP) buffer (1 × = 150 mM NaCl, 1% Triton X-100, 1 mM EDTA, 1 mM EGTA in 50 mM Tris, pH 7.4), the sample was cleared by centrifugation at 12,000 × *g* for 20 min at 4°C. The sample was then precleared with 50 μl of IgG accompanied by gentle rocking for 1 h at 4°C. Bound proteins were collected with Pierce Protein A/G Magnetic Beads and discarded. The cleared lysate was then split between two microtubes, one containing 5 μg of anti-PSD-95 (made in mouse; Millipore) and the other containing 5 μg of mouse IgG (Santa Cruz Biotechnology). Both reactions were incubated for 48 h at 4°C with gentle rocking. Bound proteins were collected with Pierce Protein A/G Magnetic Beads and washed 4 times with 1 × IP buffer. Captured protein complexes were eluted from beads with heating in Laemmli buffer at 65°C for 15 min.

Precipitates (or input, diluted threefold) were electrophoretically separated on 4–15% polyacrylamide Tris-HCl gels (Bio-Rad) at 200 V for 40 min and then transferred to nitrocellulose membranes. Blots were blocked for 1 h in blocking buffer (Rockland) and then incubated overnight at +4°C with primary antibodies diluted in blocking buffer supplemented with 0.1% Tween 20. Primary antibodies were anti-NR2A (Millipore catalog #05–901R, made in rabbit; diluted 1:5000) and anti-PSD-95 (Millipore catalog #MAB1598, made in mouse; 1:2000). The NR2A immunizing peptide shares only 35% sequence homology with the NR2B subunit, suggesting low cross-reactivity between subunits. The specificity of each antibody was confirmed by the detection of a single band at the predicted molecular weight. Blots were then washed 3 times with Tris-buffered saline (pH 7.4; TBS; Sigma-Aldrich) and incubated with IR-Dye 680LT-conjugated donkey anti-rabbit IgG (diluted 1:20,000) and IR-Dye 800CW-conjugated donkey anti-mouse IgG (diluted 1:15,000) (both secondary antibodies were purchased from LI-COR Biosciences) in 50% (v/v) blocking buffer in 0.1% Tween 20 in TBS for 1 h. Control experiments in which the primary antibodies were omitted revealed no bands, verifying the specific binding of labeled secondary antibodies. Excess antibody was removed by 3 washes of TBS with 0.1% Tween 20 followed by 3 additional washes with TBS. Blots were scanned on an Odyssey imaging system (LI-COR).

Statistical analyses. The primary measure of behavioral performance in the DRT was choice accuracy (the percentage of correct responses). For these analyses, in which rats in a given cohort (NVP, TCN, Ro 25, or ifenprodil) were microinjected with each drug dose and appropriate vehicle using a counterbalanced within-subjects design, a 2-way repeated-measures ANOVA was conducted to test the effects of dose (4 levels: vehicle and 3 doses of drug) and delay (7 levels: 0, 2, 4, 8, 12, 18, and 24 s delays). Unless otherwise noted, all data are reported as the mean ± SE. For this and all subsequent experiments, statistical analyses were conducted using SPSS 23 software and $p < 0.05$ was considered statistically significant. Significant main effects of dose were examined using Fisher's least significant difference tests to compare each dose of drug with vehicle. Dose × delay interactions were further examined using repeated-measures ANOVA that compared each dose of the drug to vehicle. Comparisons between various doses of each drug were not tested to reduce the number of comparisons. The number of trials completed in each session was analyzed by one-way ANOVA to determine whether drug administration altered non-mnemonic aspects of task performance.

Electrophysiological data were analyzed using custom software written in OriginC (OriginLab) by C.J.F. NR2B-mediated current was calculated by subtracting the average eEPSC measured in the presence of Ro 25 from the baseline response; the NR2A-mediated current was calculated by subtracting the mean eEPSC observed in Ro 25 + NVP from that obtained in Ro 25 alone. A paired-samples *t* test was used to compare the amplitude of the isolated Ro 25- and NVP-sensitive currents.

Experiment 2: Determining the relationship between excitatory signaling protein expression in aged mPFC and working memory decline

Behavioral shaping and testing. Young ($n = 8$) and aged ($n = 13$) rats were trained on the DRT described above. Rats were trained on the final set of delays for at least 1 week before obtaining performance measures used for comparisons of mPFC protein expression.

Homogenate preparation. Two weeks after testing, rats were decapitated, the brains were extracted from the skull, and the mPFC was dissected from surrounding tissues on an ice-cold plate. Dissected samples were stored at −80°C until tissue was harvested from all animals in the study. Homogenates were prepared from microdissected mPFC according to our previously published methods (McQuail et al., 2012; Bañuelos et al., 2014). Frozen mPFC samples were weighed and homogenized in 10 volumes of ice-cold buffer (1 mM EDTA, 1 mM EGTA in 50 mM HEPES, pH 7.4; reagents purchased from Sigma-Aldrich) supplemented with Halt protease inhibitors and centrifuged at 10,000 × *g* for 20 min at 4°C. The supernatant, comprising soluble proteins, was retained and the insoluble pellet, comprising the membrane fraction, was resuspended in 40 ml of the same buffer and incubated on ice for 30 min. Membranes were sedimented by centrifugation at 32,500 × *g* for 10 min and resuspended in 1 volume of 50 mM HEPES, pH 7.4. Aliquots were stored at −80°C until used for Western blotting. Protein concentrations of all samples were determined by the Pierce Coomassie (soluble fraction) or BCA (membrane fraction) protein assay kit (both from Fisher Scientific).

SDS-PAGE and immunoblotting. Proteins were denatured and reduced in Laemmli sample buffer with 5% (v/v) β-mercaptoethanol (bioWORLD) and heated at 95°C for 5 min. Unless otherwise noted, all equipment and reagents used for gel electrophoresis were purchased

Table 1. Antibodies used for immunoblotting

Target	Made in	Supplier	Part no.	Dilution
GAPDH	Rb	Santa Cruz Biotechnology	sc-25778	2000
GluR1	Rb	Millipore	ABN241	1000
GluR2	Ms	Millipore	MABN71	5000
MAP2	Rb	Millipore	AB5622	2000
NR1	Rb	Millipore	AB9864	2000
NR2A	Rb	Millipore	05-901R	5000
NR2B	Ms	Millipore	05-920	2000
PSD-95	Ms	Millipore	MAB1598	2000
Spinophilin	Rb	Millipore	06-852	2000
VGluT1	Ms	Millipore	MAB5502	1000

Rb, Rabbit; Ms, mouse.

from Bio-Rad and all steps were performed at room temperature. Five micrograms of protein per lane were electrophoretically separated on 4–15% polyacrylamide Tris-HCl gels at 200 V for 40 min and then transferred to nitrocellulose membranes. Blots were blocked for 1 h in Rockland blocking buffer and then incubated overnight at 4°C with primary antibodies (for details, see Table 1) diluted in blocking buffer supplemented with 0.1% Tween 20. The specificity of each antibody was confirmed by the detection of a single band at the predicted molecular weight. The dilution used for each antibody was optimized independently to produce a linear range of detection for 1.25–10 μg of total mPFC protein. Blots were then washed 3 times with Tris-buffered saline (pH 7.4; TBS; Sigma-Aldrich) and incubated with IR-Dye 680LT-conjugated donkey anti-rabbit IgG (diluted 1:20,000) and IR-Dye 800CW-conjugated donkey anti-mouse (diluted 1:15,000) (both secondary antibodies were purchased from LI-COR Biosciences) in 50% (v/v) blocking buffer in 0.1% Tween 20 in TBS for 1 h. Excess antibody was removed by 3 washes of TBS with 0.1% Tween 20 followed by 3 additional washes with TBS. Blots were scanned on an Odyssey imaging system (LI-COR). Samples were replicated on different gels, counterbalanced across lanes, for a total of four separate replications/sample. In addition to detection of specific proteins of interest, all blots were probed for GAPDH to ensure equality of loading across samples and experiments (independent-samples *t* tests comparing GAPDH in young versus aged: ($t_{(19)} = -0.864–0.141$, $p = 0.248–0.889$; data not shown). The intensity of immunoreactive bands was measured using ImageStudio software. Technical replicates were averaged for each sample and raw intensities were transformed to percentage protein level of young (i.e., mean expression of young = 100%).

Statistical analysis. To compare working memory abilities of young and aged rats, a 2-factor mixed measures ANOVA testing age as a between-subjects factor (2 levels: young adult or aged) and delay as a within-subjects factor (7 levels: 0, 2, 4, 8, 12, 18, and 24 s delays) was conducted on data averaged across the last 5 d of performance in the DRT. Because performance at shorter delays (0–4 s) was >90% correct in both age groups, accuracy at 8, 12, 18, and 24 s was averaged for each rat to provide the individualized measure of DRT choice accuracy for use in correlational analyses. Independent-samples *t* tests were used to compare young and aged choice accuracy and mPFC expression of proteins of interest. Relationships between protein expression and choice accuracy were tested using Pearson's *r* correlation coefficient. To avoid conflating the effects of age on behavioral and molecular measures in these analyses, a standard bivariate correlation was performed only in the aged group.

Experiment 3: Determining whether enhancement of NR2A-NMDAR signaling in aged mPFC improves working memory performance in aged rats

Electrophysiology methods. Acute mPFC tissue slices were prepared from $n = 6$ aged rats using the same procedures described in Experiment 1 above. Baseline was established in the presence of NBQX (10 μM) and Ro 25 (1 μM) to block AMPARs and NR2B-NMDARs, respectively. After 10 min, the D-amino acid oxidase (DAAO) inhibitor 3-methylpyrazole-5-carboxylic acid (MPC; Sigma-Aldrich, catalog # 644927) was added to the bath for 20 min at a concentration of 10 μM. By inhibiting the enzymatic activity of DAAO, MPC increases levels of serine, an endogenous NMDAR coagonist that is localized to the synaptic cleft (Adage et al., 2008; Papouin et al., 2012). Finally, 0.4 μM NVP was added for 15 min to block NR2A-NMDARs.

Surgical and behavioral testing procedures. Aged rats ($n = 11$) received surgery to implant guide cannulae into the mPFC exactly as described above in Experiment 1. After recovery from surgery, aged rats were trained on the DRT at the final set of delays for at least 1 week before drug testing as in Experiment 1.

Drug microinjections. Microinjection procedures were identical to those described in Experiment 1. MPC was initially dissolved in pure DMSO before dilution with aCSF to doses of 0.1, 1, and 10 μg per 0.5 μl in 20% DMSO in aCSF. To our knowledge, no studies have investigated the behavioral effects of intracerebral microinjection of MPC; however, intrathecal injection of 3 or 10 μg MPC attenuates sensitivity to pain after either sleep deprivation or formalin injection, suggesting that this range of doses produces physiologically and behaviorally detectible effects in neural tissues (Gong et al., 2011; Wei et al., 2013).

Histological verification of cannula placements. After completion of behavioral testing, rats were killed and perfused as described in Experiment 1 for histological verification of cannula placements. Cannula tip placements were visualized using a microscope under conventional bright-field illumination and mapped onto standardized coronal sections of the rat brain (Paxinos and Watson, 2005). Only those rats with placements found to terminate within the boundaries of the prelimbic or infralimbic cortex were included in the behavioral analysis. Locations of cannula placements are shown in Figure 8.

Data analysis. Electrophysiological data were analyzed using one-sample *t* tests that compared the normalized post-MPC and post-NVP responses (eEPSC amplitude or area under the curve) to test value = 1 (i.e., no change from baseline). Behavioral data in Experiment 3 were analyzed using the same procedures as in Experiment 1.

Results

Experiment 1: NR2A-containing, but not NR2B-containing, NMDARs in mPFC are critical for working memory

Behavioral pharmacology

Intra-mPFC administration of the NR2A-preferring antagonist NVP-AAM077 (NVP) significantly reduced DRT choice accuracy (main effect of dose: $F_{(3,24)} = 7.683$, $p = 0.001$; Fig. 2*B*) in a non-delay-dependent manner (dose × delay: $F_{(18,144)} = 0.578$, $p = 0.911$). *Post hoc* comparisons determined that choice accuracy was lower at all doses tested compared with vehicle (0.3 μg NVP: $p = 0.018$; 1 μg NVP: $p = 0.006$; 3 μg NVP $p = 0.002$). Intra-mPFC administration of the NR2A-selective antagonist TCN-201 (TCN) also impaired accuracy (main effect of dose: $F_{(3,30)} = 4.105$, $p = 0.016$; Fig. 2*D*), albeit in a delay-dependent fashion (dose × delay: $F_{(18,180)} = 1.740$, $p = 0.036$). *Post hoc* 2-way repeated-measures ANOVAs determined that each dose impaired accuracy compared with vehicle (main effects of dose; 0.23 fg of TCN: $p = 0.005$; 2.3 fg of TCN: $p = 0.009$; 23 fg of TCN: $p = 0.023$). A significant interaction with delay was detected after injection of 23 fg of TCN ($p = 0.005$) and a trend toward an interaction with delay was detected after injection of 0.23 fg of TCN ($p = 0.058$); a dose × delay interaction was not detected after injection of 2.3 fg of TCN ($p = 0.156$).

To determine whether these NR2A antagonists influenced non-mnemonic aspects of task performance, the number of trials completed was also analyzed. NVP modestly but reliably reduced the number of completed trials ($F_{(3,24)} = 3.864$, $p = 0.022$). *Post hoc* comparisons determined that, compared with vehicle (119 ± 3 trials), rats completed fewer trials after infusion with 0.3 μg of NVP (111 ± 5 trials, $p = 0.030$) or 3 μg of NVP (103 ± 6 trials, $p = 0.022$), but not 1 μg of NVP (115 ± 5 trials, $p = 0.453$). In contrast, TCN did not influence the number of trials completed ($F_{(3,30)} = 0.632$, $p = 0.582$; data not shown). The non-mnemonic impairments induced by NVP, especially those observed at

higher doses (non-delay-dependent impairment in accuracy, reduced trial completion rate), may be due to off-target effects that influence processes other than working memory. In fact, the highest dose of NVP (3 μg) impairs accuracy even at the 0 s delay (97.93 ± 0.86% vs 80.98 ± 4.00%; paired t test, $t_{(8)} = 3.397$, $p = 0.009$). The more selective NR2A antagonist TCN, however, impairs accuracy in a delay-dependent fashion without influencing non-mnemonic aspects of performance. Overall, these data provide strong evidence that selective NR2A blockade impairs working memory.

In marked contrast to the impairing effects of NR2A antagonists, intra-mPFC administration of two NR2B-selective antagonists, Ro 25–6981 (Ro 25; Fig. 3*B*) and ifenprodil (Fig. 3*D*), failed to affect DRT performance. Neither NR2B antagonist produced a main effect of dose (Ro 25: $F_{(3,30)} = 1.031$, $p = 0.393$; ifenprodil: $F_{(3,24)} = 0.310$, $p = 0.818$) or a dose × delay interaction (Ro 25: $F_{(18,180)} = 0.335$, $p = 0.995$; ifenprodil: $F_{(18,144)} = 0.861$, $p = 0.627$). Notably, similar doses have been shown previously to impair other aspects of mPFC-dependent behavior (Laurent and Westbrook, 2008; Sotres-Bayon et al., 2009; Brigman et al., 2013; Davies et al., 2013). Neither Ro 25 ($F_{(3,30)} = 0.634$ $p = 0.297$, data not shown) nor ifenprodil ($F_{(3,24)} = 0.615$, $p = 0.612$, data not shown) influenced the number of completed trials. Considered alongside the impairing effects of NR2A-preferring antagonists, these NR2B-selective antagonist data collectively suggest that mPFC NR2A, but not NR2B, containing, NMDARs are predominant mediators of working memory.

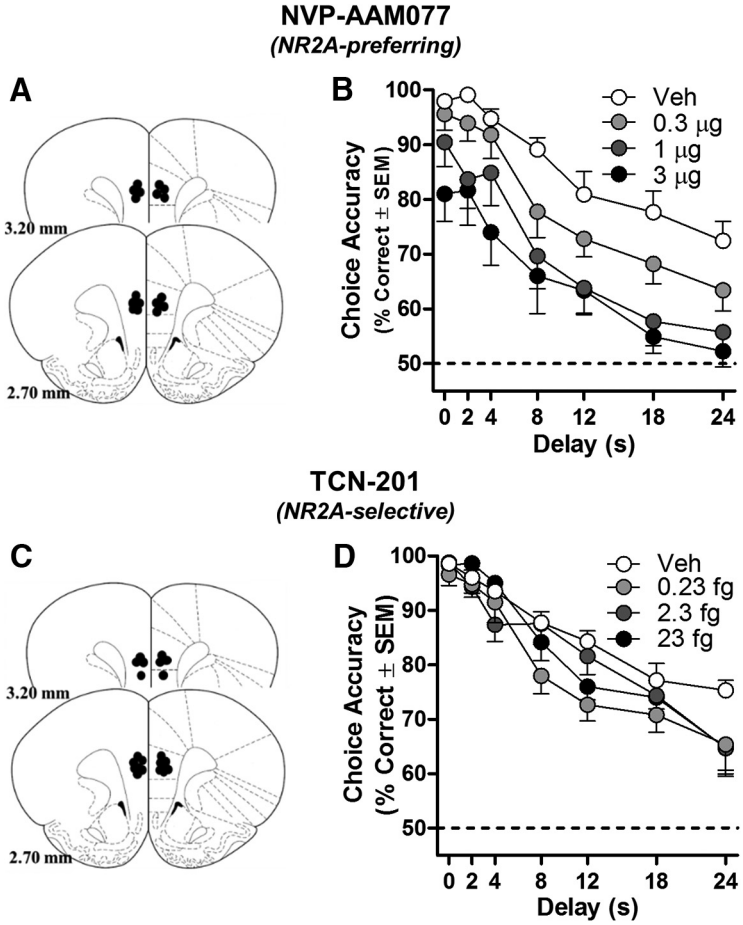

Figure 2. Blocking mPFC NR2A-NMDARs impairs working memory in rats. ***A***, ***C***, Placements of cannulae in mPFC of each rat included in this experiment (schematic illustration modified from Paxinos and Watson, 2005). Intra-mPFC microinjections of NR2A-preferring antagonists NVP ($n = 9$; ***B***) and TCN ($n = 11$; ***D***) significantly impaired accuracy on the DRT relative to vehicle; main effects of dose of NVP or TCN: $p < 0.05$. All individual doses of NVP or TCN are significantly different from their respective vehicle ($p < 0.01$–0.05). Data are mean percentage correct choices (y-axis) ± SEM plotted as a function of delay (in seconds; x-axis) and dose (separate lines).

Electrophysiology

Given these findings and the role of persistent pyramidal neuron activity in working memory (Goldman-Rakic, 1995; Wang et al., 2013), it could be predicted that NR2A receptors are significant contributors to NMDAR currents on mature pyramidal neurons. Figure 4, *A–C*, shows representative and averaged NMDAR-eEPSCs recorded from L2/3 mPFC pyramidal neurons under baseline conditions and after sequential application of Ro 25 and NVP to isolate the NR2B and NR2A-mediated components of the NMDAR-eEPSC. Across 10 cells, only 21.4 ± 5.5% of the total NMDAR-eEPSC was blocked by Ro 25, whereas 78.6 ± 5.5% was blocked by subsequent NVP application ($t_{(9)} = 5.219$, $p = 5.50\text{E-}4$, $n = 10$ cells; Fig. 4*D*). The pronounced contribution of NR2A-NMDARs to the eEPSC may reflect the preferential localization of NR2A-NMDARs to the synaptic zone (Townsend et al., 2003; Groc et al., 2006), where they would be well positioned to summate synaptic inputs necessary for persistent firing and, by extension, working memory. To verify synaptic localization of NR2A in the mPFC, protein complexes were immunoprecipitated from mPFC homogenates using an antibody against PSD-95, the synaptic NMDAR scaffold. Precipitates were subsequently probed for NR2A, revealing its physical association with PSD-95 in the mPFC (Fig. 4*E*). Control reactions substituting an irrelevant IgG for anti-PSD-95 validated the specificity of these protein:protein interactions. Collectively, data from electrophysiology and coimmunoprecipitation studies strongly suggest that the majority of NMDARs in cortical pyramidal neurons contain at least one NR2A subunit and that this subunit is found at synaptic sites in the mPFC.

Experiment 2: Reduced NR2A expression in mPFC correlates with age-related working memory decline

In agreement with previous findings (Beas et al., 2013; Bañuelos et al., 2014), Figure 5*A* shows that DRT performance of aged rats is less accurate than that in young rats, particularly at longer delays (age × delay interaction: $F_{(6,114)} = 3.813$, $p = 0.002$). Indeed, both young and aged rats demonstrate a high degree of accuracy (>90% correct) at short delays (0–4 s), whereas aged rats show disproportionate reductions in accuracy at longer delays. It is notable that, as shown in Figure 5*B*, not all aged rats were impaired to the same degree and some maintained performance on par with the young cohort. Figure 6*A* shows representative expression of excitatory signaling proteins evaluated by Western blot in homogenates prepared from microdissected mPFC from these rats. As shown in Figure 6*B*, expression of the NMDAR

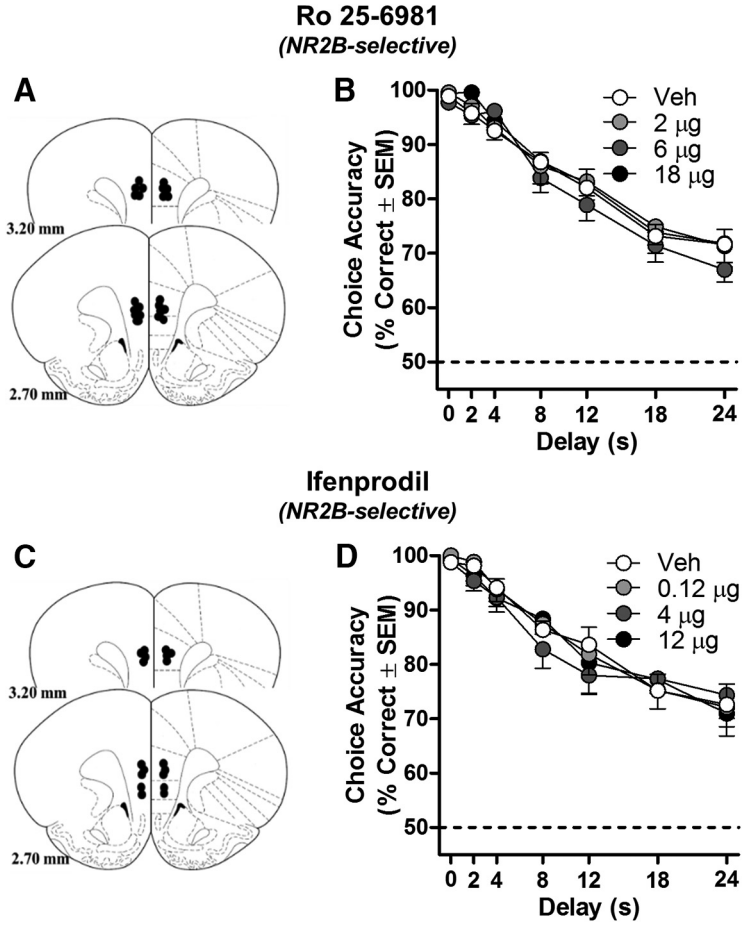

Figure 3. Blocking mPFC NR2B-NMDARs does not influence working memory in rats. ***A***, ***C***, Placements of cannulae in mPFC of each rat included in this experiment (schematic illustration modified from Paxinos and Watson, 2005). Intra-mPFC microinjections of NR2B-selective antagonists Ro 25 ($n = 11$; ***B***) and ifenprodil ($n = 9$; ***D***) did not influence DRT choice accuracy. Data are mean percentage correct choices (*y*-axis) ± SEM plotted as a function of delay (in seconds; *x*-axis) and dose (separate lines).

subunits NR1 ($t_{(19)} = 2.200, p = 0.040$), NR2A ($t_{(19)} = 2.174, p = 0.043$), and NR2B ($t_{(19)} = 2.853$, $p = 0.010$) was significantly reduced with age. In contrast, expression of AMPA receptor subunits in the same cohort was only marginally and not reliably reduced (GluR1: $t_{(19)} = 1.971$, $p = 0.064$; GluR2: $t_{(19)} = 1.780$, $p = 0.091$). Bivariate correlations were performed on individual data from aged rats to determine whether protein expression was associated with mean DRT choice accuracy (data plotted in Fig. 5*B*). This analysis revealed a significant, positive association between working memory performance and NR2A ($r = 0.66$, $p = 0.01$; Fig. 7*B*), but not for any of the other receptor subunits examined ($r = -0.04$–0.42, $p = 0.15$–0.75; Fig. 7). Notably, the relationship between NR2A and impaired working memory did not appear secondary to an overall loss of excitatory synapses. Aging did not influence the expression of PSD-95, spinophilin, or MAP2 ($t_{(19)} = 0.35$–1.69, $p = 0.107$–0.729; Fig. 6*D*), surrogate markers of postsynaptic density, spines, and dendrites, respectively. Although the expression of vesicular glutamate transporter 1 (VGluT1), a cortex-specific marker of excitatory terminals, was significantly reduced with age ($t_{(19)} = 2.352$, $p = 0.030$; Fig. 6*D*), attenuated VGluT1 expression was not associated with choice accuracy ($r = -0.043$, $p = 0.888$; Fig. 7*F*) or NR2A expression ($r = -0.16$, $p = 0.597$; data not shown).

Experiment 3: Blocking serine breakdown in the mPFC prolongs NR2A-NMDAR activity and enhances working memory in aged rats

Electrophysiology

If the reduced NR2A expression reported here is a critical mediator of working memory impairment in aged rats, it might be predicted that enhancing activity at remaining NR2A-NMDARs in the mPFC of aged rats should improve working memory performance. NR2A-specific agonists suitable for use *in vivo* do not currently exist; however, as described above, the importance of NR2A-NMDARs to working memory may be attributable to their primary localization at synaptic sites where they are well positioned to mediate recurrent excitation (Fig. 4*E*, Tovar and Westbrook, 1999; Townsend et al., 2003; Erreger et al., 2005; Groc et al., 2006). Recent *in vitro* electrophysiological data indicate that serine acts preferentially as an endogenous coagonist at synaptic NMDARs, whereas glycine preferentially occupies this site on extrasynaptic NMDARs (Papouin et al., 2012). Based on these findings, *in vitro* electrophysiological experiments were performed in the current study to determine whether increasing endogenous serine with a DAAO inhibitor specifically enhances NR2A-NMDAR activity in aged rat mPFC. In acute slices, NR2A-NMDAR-eEPSCs were isolated with the addition of antagonists to AMPA and NR2B-NMDARs. Evoked EPSCs were measured both before and after the application of MPC, a DAAO inhibitor that prevents the degradation of endogenous serine. Figure 8 shows that bath application of MPC significantly enhances the area of the NMDAR-mediated eEPSC in the presence of both DNQX and Ro 25 ($t_{(11)} = 2.658$, $p = 0.022$). The subsequent inhibition by NVP ($t_{(11)} = 13.498$, $p < 0.001$) further indicates that this effect is likely mediated by increased charge transfer through NR2A-containing receptors capable of responding to synaptically released glutamate.

Behavioral pharmacology

Figure 8*D* shows the performance of aged rats after intra-mPFC administration of MPC. MPC significantly enhanced performance of aged rats in a delay-dependent manner (dose × delay interaction: $F_{(18,180)} = 1.857$, $p = 0.022$). *Post hoc* comparisons with vehicle performance determined that 1 μg of MPC significantly improved aged rat performance in a delay-dependent fashion ($F_{(6,60)} = 4.321$, $p = 0.001$). Performance after 0.1 μg MPC and 10 μg MPC doses did not reliably differ from vehicle (main effect of dose: $F = 0.642$–1.374, $p = 0.268$–0.442; dose × delay: $F = 0.373$–1.344, $p = 0.252$–0.893). MPC did not affect the number of trials completed ($F_{(3,30)} = 0.708$, $p = 0.555$), suggesting that the behavioral improvement observed with the 1 μg dose of MPC was not due to effects on non-mnemonic aspects of task performance.

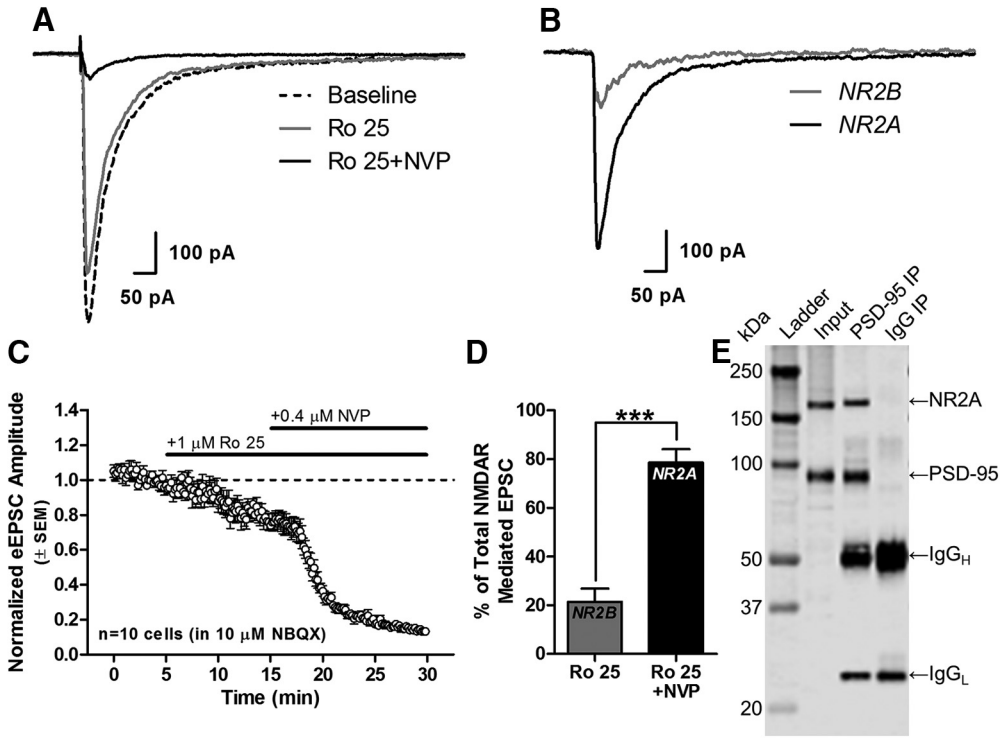

Figure 4. NR2A-NMDARs are major contributors to eEPSCs on L2/3 pyramidal neurons and associate with synaptic scaffolds in rat mPFC. ***A***, Representative NMDAR-eEPSCs from a L2/3 pyramidal neuron in the mPFC at baseline (predrug) and after addition of 1 μM Ro 25 and Ro 25 + 0.4 μM NVP. Each trace shown is an average of 18 individual traces recorded consecutively over a 3 min period in the stated conditions. ***B***, Subtraction of raw traces (baseline − Ro 25, and Ro 25 − NVP) reveals the isolated NR2B- and NR2A-mediated components of the eEPSC, respectively. ***C***, Population data ($n = 10$ cells from 7 rats) over time illustrating the effect of Ro 25 and NVP on eEPSC amplitude. ***D***, Summary data indicating the percentage of the total NMDAR-eEPSC that is blocked by Ro 25 and NVP (after subtraction of Ro 25). Error bars represent SEM. ***$p < 0.001$. ***E***, When a PSD-95-specific antibody was used to immunoprecipitate protein complexes from mPFC homogenates ($n = 3$ rats, pooled), NR2A is present in the precipitate ("PSD-95 IP"). As a negative control, an irrelevant IgG did not precipitate either PSD-95 or NR2A ("IgG IP").

Discussion

Contributions of NR2A- and NR2B-containing NMDARs to working memory

To our knowledge, this study is the first to empirically differentiate the individual contributions of NR2A-NMDARs and NR2B-NMDARs in PFC to working memory. Significant impairments in choice accuracy were observed in young rats after acute blockade of NR2A in the mPFC by local infusion of either the NR2A-preferring antagonist NVP (Auberson et al., 2002; Frizelle et al., 2006; Neyton and Paoletti, 2006) or the more selective NR2A antagonist TCN (Bettini et al., 2010; Edman et al., 2012; Hansen et al., 2012). This finding contrasts with a prior study that investigated NMDAR subtype contributions to DRT performance using systemic drug administration. In this prior study, NVP had no effect, but the NR2B antagonist Ro 25 impaired choice accuracy (Smith et al., 2011). Notably, however, a second NR2B-selective antagonist (CP 101–606) tested in the same study failed to impair performance. Moreover, systemic administration of these drugs induced significant changes in non-mnemonic measures of performance (Smith et al., 2011), complicating the ability to isolate effects on PFC-supported cognition. Intra-mPFC administration of NR2A antagonists in the current study produced no (TCN) or very modest (NVP) effects on non-mnemonic performance measures, and choice accuracy was unchanged after intra-mPFC administration of Ro 25 or ifenprodil two highly selective NR2B antagonists (Gallagher et al., 1996; Fischer et al., 1997). Importantly, even the lowest doses tested for both Ro 25 and ifenprodil were reported previously to impair other forms of mPFC-dependent cognition, including odor span memory, reversal learning, fear conditioning, and extinction learning (Laurent and Westbrook, 2008; Sotres-Bayon et

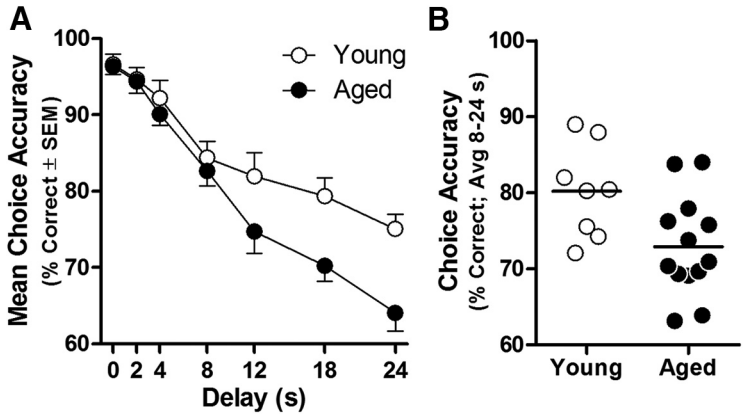

Figure 5. DRT performance in young and aged rats. ***A***, DRT choice accuracy of aged rats ($n = 13$; black circles) is reduced relative to young ($n = 8$; white circles) at longer delays (age × delay interaction: $p < 0.05$). Data are mean percentage correct choices (y-axis) ± SEM plotted as a function of delay (in seconds; x-axis). ***B***, Choice accuracy (averaged across 8, 12, 18, and 24 s delays) of individual young and aged rats.

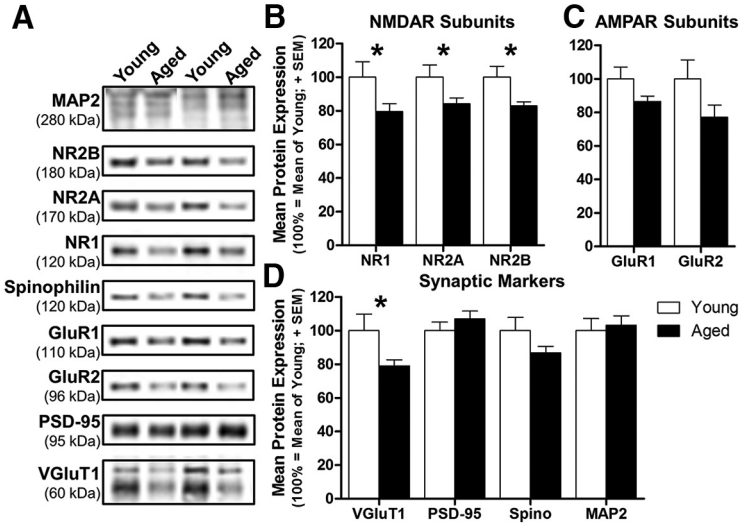

Figure 6. Expression of excitatory receptor subunits and synaptic markers in the mPFC of young and aged rats. ***A***, Representative immunoreactive bands from mPFC homogenates prepared from young and aged rats. To prepare this image, two independent pairs of immunoreactive bands (one young and one aged from adjacent lanes) were selected from each immunoblotting experiment and image acquisition/presentation parameters including laser intensity, pixel resolution, brightness, and contrast were applied equally. ***B***, Expression of NR1, NR2A, and NR2B was lower in aged compared with young rats. ***C***, GluR1 and GluR2 levels were marginally lower with age. ***D***, Although there was a significant reduction of VGluT1 in aged mPFC, levels of PSD-95, spinophilin, and MAP2 were unchanged. ***B–D***, Protein expression (100% = mean expression of young group; *y*-axis) of young ($n = 8$; white bars) and aged ($n = 13$; black bars); $^*p < 0.05$.

slower channel kinetics of NR2B make this subunit particularly well suited to support the excitatory dynamics of dorsolateral PFC (dlPFC) pyramidal neurons necessary for maintaining information in working memory stores (Wang et al., 2008). Although some characteristics of the highly evolved primate dlPFC are not necessarily present in the rodent mPFC (Caetano et al., 2012), other previous reports from both nonhuman primate and rat (Liu et al., 2007; Gonzalez-Burgos et al., 2008; Wang et al., 2008) agree with the electrophysiological data reported here demonstrating that NR2B-NMDAR blockade only partially reduces NMDAR-eEPSC amplitude on L2/3 pyramidal neurons in young PFC. Significantly, the current study is the first to show that subsequent application of NVP at a dose that preferentially inhibits NR2A-NMDARs (Liu et al., 2004; Massey et al., 2004) blocks the majority (~80%) of the NMDAR-eEPSC, indicating a predominant role for the NR2A subunit in modulating pyramidal neuron excitability. Indeed, among the various features that specify contributions of NR2A to neural function and cognition, the most pertinent may be its stable localization within the synaptic zone (Townsend et al., 2003; Groc et al., 2006). At this location, NR2A-NMDARs are well positioned to summate a variety of synaptic inputs necessary to support the persistent firing required for working memory. Although the electrophysiological measures used here do not

al., 2009; Brigman et al., 2013; Davies et al., 2013). In the current study, working memory accuracy was unchanged even at doses of Ro 25 and ifenprodil that were an order of magnitude higher those used in these previous studies.

The failure of intra-mPFC NR2B antagonist administration to impair DRT performance contrasts with prior suggestions that the

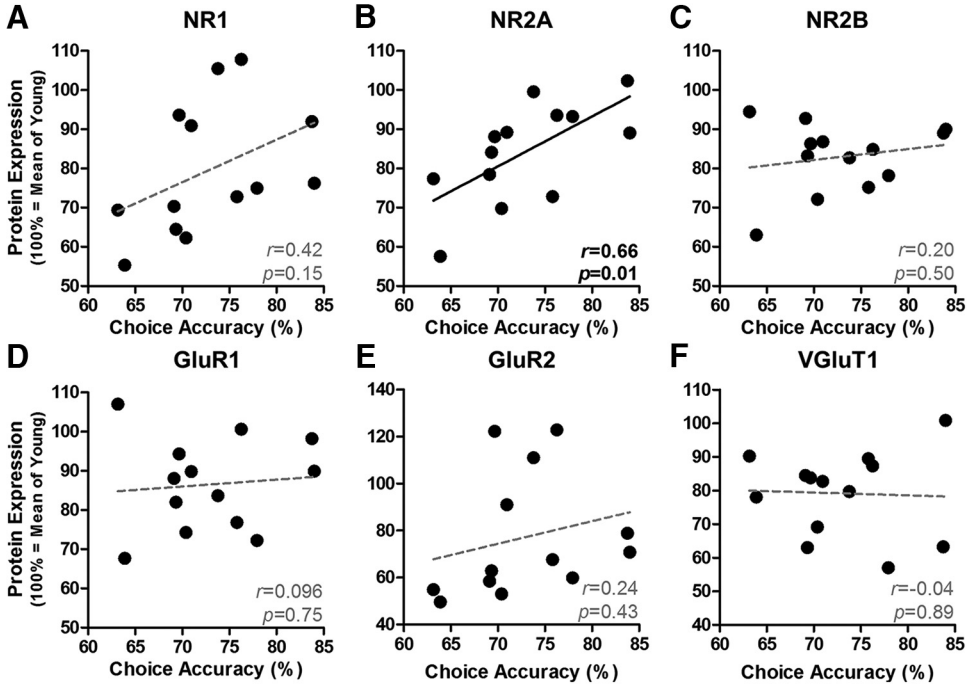

Figure 7. Relationship between mPFC protein levels and working memory performance in aged rats. ***A–C***, Among NR1, NR2A, and NR2B, only NR2A expression (***B***) is positively associated with working memory among aged rats ($n = 13$). ***D–F***, There was no relationship between level of GluR1, GluR2, or VGluT and working memory in aged rats. For all panels, each black circle represents a single aged rat plotted as a function of protein expression (100% = mean expression of young group; *y*-axis) and accuracy (percentage correct; *x*-axis) with line of best fit. Inset, Pearson's *r* and *p*.

rule out contributions of extrasynaptic receptors, a complementary biochemical experiment confirmed that NR2A-NMDARs localize to synaptic sites in mPFC by demonstrating that NR2A associates physically with the synaptic scaffolding protein PSD-95. It should be noted, however, that NR2B has been observed at synaptic sites in L3 of the monkey dlPFC (Wang et al., 2013) and partitions into the crude synaptosomal fraction of rodent mPFC homogenates, where it associates with PSD-95 and NR2A (Zamzow et al., 2013). Such synaptic NR2B may be primarily attributable to triheteromeric NMDAR complexes that contain both NR2A and NR2B. These NR1/NR2A/NR2B triheteromers have been identified in cortex (Luo et al., 1997) and exhibit reduced sensitivity to subunit-selective antagonists relative to NR1/NR2B diheteromers (Hatton and Paoletti, 2005; Hansen et al., 2014). Therefore, whereas the current data indicate that pure NR1/NR2B diheteromers play a minimal role in working memory, the possible contributions to cognition of NR2B subunits via triheteromeric complexes remain an important avenue of future study.

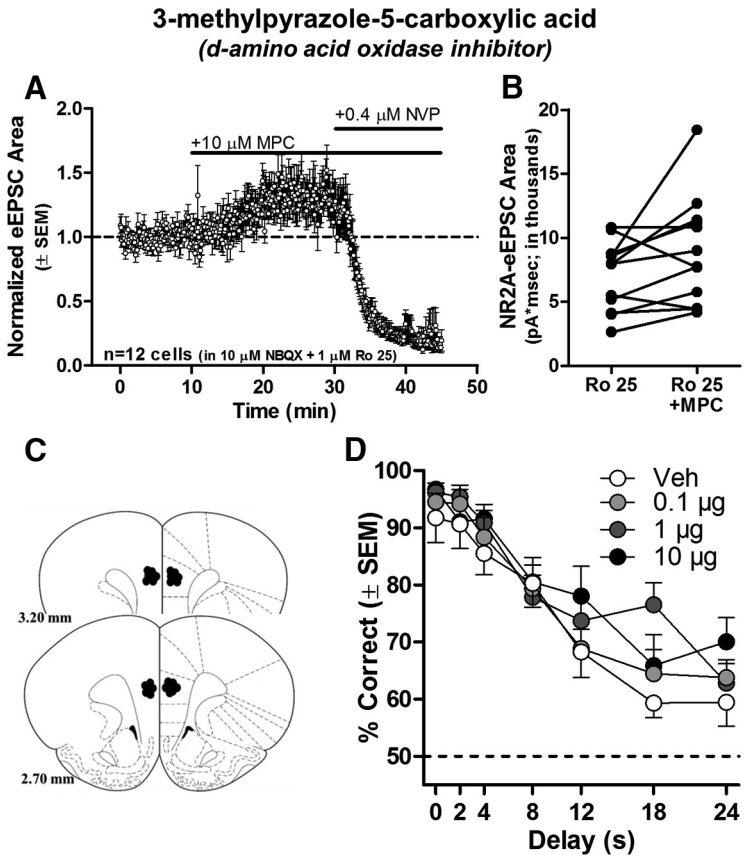

Figure 8. Potentiating synaptic mPFC NMDAR activity improves working memory in aged rats. ***A***, Population data ($n = 12$ cells from 6 aged rats) over time illustrating the effect of MPC and NVP on eEPSC area. ***B***, NMDAR-EPSC area (pA*msec) of individual cells is significantly increased by the application of MPC in the presence of Ro 25. ***C***, Placements of cannulae in mPFC of each rat ($n = 11$) included in this experiment (schematic illustration modified from Paxinos and Watson, 2005). ***D***, Intra-mPFC microinjection of MPC significantly improves choice accuracy relative to vehicle in a delay-dependent manner (dose × delay interaction: $p < 0.05$). Data are mean percentage correct choices (*y*-axis) ± SEM plotted as a function of delay (in seconds; *x*-axis) and dose (separate lines).

Relevance of NR2A to age-related working memory impairment and its treatment

The current findings demonstrate that reduced expression of NR2A is a key molecular correlate of age-related working memory impairment, a finding that has implications for therapeutic approaches designed to rescue cognition at advanced ages. In agreement with prior findings across species (Oscar-Berman and Bonner, 1985; Dunnett et al., 1988; Rapp and Amaral, 1989; Bachevalier et al., 1991; Lamar and Resnick, 2004; Beas et al., 2013), working memory performance of aged rats in the current study was significantly less accurate than that of young, particularly as the delay interval during which they were required to remember the correct response lever increased. The finding of significant age-related reductions detected across all NMDAR subunits corroborates prior molecular, biochemical, and physiological findings in aged mPFC (Magnusson, 2000; but see Sonntag et al., 2000; Magnusson et al., 2002; Liu et al., 2008; Zhao et al., 2009; Zamzow et al., 2013; Guidi et al., 2015). It is also notable that the age-related reduction in VGluT1 expression agrees with substantial prior evidence indicating that excitatory synapse loss is a consistent feature of PFC aging (Masliah et al., 1993; Peters et al., 2008; Dumitriu et al., 2010; Bloss et al., 2013). Importantly, the current study is the first to report that reduced NR2A expression in mPFC may be particularly critical for mediating working memory impairment among aged subjects. Indeed, NR2A was the sole excitatory signaling protein examined that reliably associated with working memory ability in aging. In contrast, individual differences in NR2B, AMPAR subunits, and a variety of surrogate markers of synaptic integrity did not relate to working memory ability among aged rats. This pattern of results makes it highly unlikely that the relationship between NR2A and working memory in aged rats is mediated simply by excitatory synapse loss. Nevertheless, age-related reductions in excitatory synapses may interact with decline in affiliated signaling elements observed here to exacerbate working memory impairments (Dyall et al., 2007; Majdi et al., 2009; Dumitriu et al., 2010; Bloss et al., 2013). Future experiments are required to elucidate the full nature of excitatory signaling alterations that contribute to age-related cognitive decline.

The relationship between reduced mPFC NR2A expression and working memory decline in aged rats implicates enhancement of NR2A-NMDAR activity as a strategy for improving cognition in aged rats. With no available NR2A-selective potentiators suitable for use *in vivo*, we pursued the hypothesis that the importance of NR2A-NMDARs in working memory is attributable to their primary localization at synaptic sites (Fig. 4*E* and also Tovar and Westbrook, 1999; Townsend et al., 2003; Erreger et al., 2005; Groc et al., 2006). Serine is an endogenous NMDAR coagonist that is enriched in the synaptic cleft, where NR2A-NMDARs are most prevalent (Mothet et al., 2000; Papouin et al., 2012). Inhibition of DAAO should thus promote serine availability preferentially at NR2A-enriched synaptic NMDARs. Consistent with this rationale, we demonstrated that the DAAO inhibitor MPC prolongs synaptically evoked NR2A-NMDAR activity on aged mPFC pyramidal neurons. As mentioned previously, cellular models of working memory posit that prolonged NMDAR signaling is advantageous to working memory because it affords greater opportunity to integrate excitatory inputs and sustain persistent firing (Goldman-Rakic, 1995; Wang et al., 2013). Indeed,

when MPC was infused into the mPFC of aged rats, working memory was significantly improved. These data strongly suggest that potentiation of synaptic NR2A-NMDARs comprises a feasible approach to rescue depressed PFC neural activity and working memory. Future work in which MPC is coadministered with other NR2 subtype antagonists will nevertheless be important to verify the precise mechanism by which this compound acts *in vivo* to improve working memory. Alternatively, novel NR2A-selective positive allosteric modulators were recently synthesized and characterized *in vitro* (Hackos et al., 2016). Although not yet optimized for use *in vivo*, such a class of drugs could provide more selective and reliable potentiation of NR2A over the indirect methods used here and elsewhere (Dunlop and Brandon, 2015) to ultimately achieve more substantial rescue of cognition in aging and disease states.

Conclusion

Although current theories favor contributions from NR2B-NMDARs to PFC neural physiology and working memory, here we provide converging evidence that NR2A-NMDARs are necessary for working memory and associate with cognitive status in aging. These new findings should direct future studies toward further investigation of the properties and contributions of NR2A to normal neural function and cognition. A better understanding of the role of NR2A-NMDARs in PFC may advance treatment options for cognitive impairment in conditions associated with altered PFC glutamatergic neurotransmission, including normal aging and neuropsychiatric conditions such as schizophrenia.

References

Adage T, Trillat AC, Quattropani A, Perrin D, Cavarec L, Shaw J, Guerassimenko O, Giachetti C, Gréco B, Chumakov I, Halazy S, Roach A, Zaratin P (2008) In vitro and in vivo pharmacological profile of AS057278, a selective d-amino acid oxidase inhibitor with potential anti-psychotic properties. Eur Neuropsychopharmacol 18:200–214. CrossRef Medline

Auberson YP, Allgeier H, Bischoff S, Lingenhoehl K, Moretti R, Schmutz M (2002) 5-Phosphonomethylquinoxalinediones as competitive NMDA receptor antagonists with a preference for the human 1A/2A, rather than 1A/2B receptor composition. Bioorg Med Chem Lett 12:1099–1102. CrossRef Medline

Bachevalier J, Landis LS, Walker LC, Brickson M, Mishkin M, Price DL, Cork LC (1991) Aged monkeys exhibit behavioral deficits indicative of widespread cerebral dysfunction. Neurobiol Aging 12:99–111. CrossRef Medline

Baddeley AD (1986) Working memory. Oxford: OUP.

Bañuelos C, Beas BS, McQuail JA, Gilbert RJ, Frazier CJ, Setlow B, Bizon JL (2014) Prefrontal cortical GABAergic dysfunction contributes to age-related working memory impairment. J Neurosci 34:3457–3466. CrossRef Medline

Barria A, Malinow R (2002) Subunit-specific NMDA receptor trafficking to synapses. Neuron 35:345–353. CrossRef Medline

Beas BS, Setlow B, Bizon JL (2013) Distinct manifestations of executive dysfunction in aged rats. Neurobiol Aging 34:2164–2174. CrossRef Medline

Bettini E, Sava A, Griffante C, Carignani C, Buson A, Capelli AM, Negri M, Andreetta F, Senar-Sancho SA, Guiral L, Cardullo F (2010) Identification and characterization of novel NMDA receptor antagonists selective for NR2A- over NR2B-containing receptors. J Pharmacol Exp Ther 335:636–644. CrossRef Medline

Bloss EB, Puri R, Yuk F, Punsoni M, Hara Y, Janssen WG, McEwen BS, Morrison JH (2013) Morphological and molecular changes in aging rat prelimbic prefrontal cortical synapses. Neurobiol Aging 34:200–210. CrossRef Medline

Brigman JL, Daut RA, Wright T, Gunduz-Cinar O, Graybeal C, Davis MI, Jiang Z, Saksida LM, Jinde S, Pease M, Bussey TJ, Lovinger DM, Nakazawa K, Holmes A (2013) GluN2B in corticostriatal circuits governs choice learning and choice shifting. Nat Neurosci 16:1101–1110. CrossRef Medline

Burke SN, Barnes CA (2010) Senescent synapses and hippocampal circuit dynamics. Trends Neurosci 33:153–161. CrossRef Medline

Caetano MS, Horst NK, Harenberg L, Liu B, Arnsten AF, Laubach M (2012) Lost in transition: aging-related changes in executive control by the medial prefrontal cortex. J Neurosci 32:3765–3777. CrossRef Medline

Davies DA, Greba Q, Howland JG (2013) GluN2B-containing NMDA receptors and AMPA receptors in medial prefrontal cortex are necessary for odor span in rats. Front Behav Neurosci 7:183. CrossRef Medline

Dumitriu D, Hao J, Hara Y, Kaufmann J, Janssen WG, Lou W, Rapp PR, Morrison JH (2010) Selective changes in thin spine density and morphology in monkey prefrontal cortex correlate with aging-related cognitive impairment. J Neurosci 30:7507–7515. CrossRef Medline

Dunlop J, Brandon NJ (2015) Schizophrenia drug discovery and development in an evolving era: are new drug targets fulfilling expectations? J Psychopharmacol 29:230–238. CrossRef Medline

Dunnett SB, Evenden JL, Iversen SD (1988) Delay-dependent short-term memory deficits in aged rats. Psychopharmacology (Berl) 96:174–180. Medline

Dyall SC, Michael GJ, Whelpton R, Scott AG, Michael-Titus AT (2007) Dietary enrichment with omega-3 polyunsaturated fatty acids reverses age-related decreases in the GluR2 and NR2B glutamate receptor subunits in rat forebrain. Neurobiol Aging 28:424–439. CrossRef Medline

Edman S, McKay S, MacDonald LJ, Samadi M, Livesey MR, Hardingham GE, Wyllie DJ (2012) TCN 201 selectively blocks GluN2A-containing NMDARs in a GluN1 co-agonist dependent but non-competitive manner. Neuropharmacology 63:441–449. CrossRef Medline

Erreger K, Dravid SM, Banke TG, Wyllie DJ, Traynelis SF (2005) Subunit-specific gating controls rat NR1/NR2A and NR1/NR2B NMDA channel kinetics and synaptic signalling profiles. J Physiol 563:345–358. CrossRef Medline

Fischer G, Mutel V, Trube G, Malherbe P, Kew JN, Mohacsi E, Heitz MP, Kemp JA (1997) Ro 25–6981, a highly potent and selective blocker of N-Methyl-D-aspartate receptors containing the NR2B subunit: characterization in vitro. J Pharmacol Exp Ther 283:1285–1292. Medline

Foster TC (2012) Dissecting the age-related decline on spatial learning and memory tasks in rodent models: N-methyl-D-aspartate receptors and voltage-dependent Ca2+ channels in senescent synaptic plasticity. Prog Neurobiol 96:283–303. CrossRef Medline

Frizelle PA, Chen PE, Wyllie DJ (2006) Equilibrium Constants for (R)-[(S)-1-(4-Bromo-phenyl)-ethylamino]-(2,3-dioxo-1,2,3,4-tetrahydroquinoxalin-5-yl)-methyl]-phosphonic acid (NVP-AAM077) acting at recombinant NR1/NR2A and NR1/NR2B N-methyl-D-aspartate receptors: Implications for studies of synaptic transmission. Mol Pharmacol 70:1022–1032. CrossRef Medline

Gallagher MJ, Huang H, Pritchett DB, Lynch DR (1996) Interactions between ifenprodil and the NR2B subunit of the N-methyl-D-aspartate receptor. J Biol Chem 271:9603–9611. CrossRef Medline

Gipson CD, Reissner KJ, Kupchik YM, Smith AC, Stankeviciute N, Hensley-Simon ME, Kalivas PW (2013) Reinstatement of nicotine seeking is mediated by glutamatergic plasticity. Proc Natl Acad Sci U S A 110:9124–9129. CrossRef Medline

Goldman-Rakic PS (1995) Cellular basis of working memory. Neuron 14:477–485. CrossRef Medline

Gong N, Gao ZY, Wang YC, Li XY, Huang JL, Hashimoto K, Wang YX (2011) A series of D-amino acid oxidase inhibitors specifically prevents and reverses formalin-induced tonic pain in rats. J Pharmacol Exp Ther 336:282–293. CrossRef Medline

Gonzalez-Burgos G, Kroener S, Zaitsev AV, Povysheva NV, Krimer LS, Barrionuevo G, Lewis DA (2008) Functional maturation of excitatory synapses in layer 3 pyramidal neurons during postnatal development of the primate prefrontal cortex. Cereb Cortex 18:626–637. CrossRef Medline

Groc L, Heine M, Cousins SL, Stephenson FA, Lounis B, Cognet L, Choquet D (2006) NMDA receptor surface mobility depends on NR2A–2B subunits. Proc Natl Acad Sci U S A 103:18769–18774. CrossRef Medline

Guidi M, Kumar A, Foster TC (2015) Impaired attention and synaptic senescence of the prefrontal cortex involves redox regulation of NMDA receptors. J Neurosci 35:3966–3977. CrossRef Medline

Hackos DH, Lupardus PJ, Grand T, Chen Y, Wang TM, Reynen P, Gustafson A, Wallweber HJ, Volgraf M, Sellers BD, Schwarz JB, Paoletti P, Sheng M, Zhou Q, Hanson JE (2016) Positive allosteric modulators of GluN2A-containing NMDARs with distinct modes of action and impacts on circuit function. Neuron 89:983–999. CrossRef Medline

Hansen KB, Ogden KK, Traynelis SF (2012) Subunit-selective allosteric in-

hibition of glycine binding to NMDA receptors. J Neurosci 32:6197–6208. CrossRef Medline

Hansen KB, Ogden KK, Yuan H, Traynelis SF (2014) Distinct functional and pharmacological properties of triheteromeric GluN1/GluN2A/GluN2B NMDA receptors. Neuron 81:1084–1096. CrossRef Medline

Hatton CJ, Paoletti P (2005) Modulation of triheteromeric NMDA receptors by N-terminal domain ligands. Neuron 46:261–274. CrossRef Medline

Lamar M, Resnick SM (2004) Aging and prefrontal functions: dissociating orbitofrontal and dorsolateral abilities. Neurobiol Aging 25:553–558. CrossRef Medline

Laurent V, Westbrook RF (2008) Distinct contributions of the basolateral amygdala and the medial prefrontal cortex to learning and relearning extinction of context conditioned fear. Learn Mem 15:657–666. CrossRef Medline

Liu L, Wong TP, Pozza MF, Lingenhoehl K, Wang Y, Sheng M, Auberson YP, Wang YT (2004) Role of NMDA receptor subtypes in governing the direction of hippocampal synaptic plasticity. Science 304:1021–1024. CrossRef Medline

Liu P, Smith PF, Darlington CL (2008) Glutamate receptor subunits expression in memory-associated brain structures: regional variations and effects of aging. Synapse 62:834–841. CrossRef Medline

Liu Y, Wong TP, Aarts M, Rooyakkers A, Liu L, Lai TW, Wu DC, Lu J, Tymianski M, Craig AM, Wang YT (2007) NMDA receptor subunits have differential roles in mediating excitotoxic neuronal death both in vitro and in vivo. J Neurosci 27:2846–2857. CrossRef Medline

Luo J, Wang Y, Yasuda RP, Dunah AW, Wolfe BB (1997) The majority of N-methyl-d-aspartate receptor complexes in adult rat cerebral cortex contain at least three different subunits (NR1/NR2a/NR2b). Mol Pharmacol 51:79–86. Medline

Magnusson KR (2000) Declines in mRNA expression of different subunits may account for differential effects of aging on agonist and antagonist binding to the NMDA receptor. J Neurosci 20:1666–1674. Medline

Magnusson KR, Nelson SE, Young AB (2002) Age-related changes in the protein expression of subunits of the NMDA receptor. Brain Res Mol Brain Res 99:40–45. CrossRef Medline

Majdi M, Ribeiro-da-Silva A, Cuello AC (2009) Variations in excitatory and inhibitory postsynaptic protein content in rat cerebral cortex with respect to aging and cognitive status. Neuroscience 159:896–907. CrossRef Medline

Masliah E, Mallory M, Hansen L, DeTeresa R, Terry RD (1993) Quantitative synaptic alterations in the human neocortex during normal aging. Neurology 43:192–197. CrossRef Medline

Massey PV, Johnson BE, Moult PR, Auberson YP, Brown MW, Molnar E, Collingridge GL, Bashir ZI (2004) Differential roles of NR2A and NR2B-containing NMDA receptors in cortical long-term potentiation and long-term depression. J Neurosci 24:7821–7828. CrossRef Medline

McQuail JA, Bañuelos C, LaSarge CL, Nicolle MM, Bizon JL (2012) GABAB receptor GTP-binding is decreased in the prefrontal cortex but not the hippocampus of aged rats. Neurobiol Aging 33:1124.e1–1124.e12. CrossRef Medline

McQuail JA, Frazier CJ, Bizon JL (2015) Molecular aspects of age-related cognitive decline: the role of GABA signaling. Trends Mol Med 21:450–460. CrossRef Medline

Mothet JP, Parent AT, Wolosker H, Brady RO Jr, Linden DJ, Ferris CD, Rogawski MA, Snyder SH (2000) D-serine is an endogenous ligand for the glycine site of the N-methyl-D-aspartate receptor. Proc Natl Acad Sci U S A 97:4926–4931. CrossRef Medline

Neyton J, Paoletti P (2006) Relating NMDA receptor function to receptor subunit composition: limitations of the pharmacological approach. J Neurosci 26:1331–1333. CrossRef Medline

Oscar-Berman M, Bonner RT (1985) Matching- and delayed matching-to-sample performance as measures of visual processing, selective attention, and memory in aging and alcoholic individuals. Neuropsychologia 23:639–651. CrossRef Medline

Papouin T, Ladépêche L, Ruel J, Sacchi S, Labasque M, Hanini M, Groc L, Pollegioni L, Mothet JP, Oliet SH (2012) Synaptic and extrasynaptic NMDA receptors are gated by different endogenous coagonists. Cell 150:633–646. CrossRef Medline

Paxinos G, Watson C (2005) The rat brain in stereotaxic coordinates. New York: Elsevier Academic.

Peters A, Sethares C, Luebke JI (2008) Synapses are lost during aging in the primate prefrontal cortex. Neuroscience 152:970–981. CrossRef Medline

Rapp PR, Amaral DG (1989) Evidence for task-dependent memory dysfunction in the aged monkey. J Neurosci 9:3568–3576. Medline

Sans N, Petralia RS, Wang YX, Blahos J 2nd, Hell JW, Wenthold RJ (2000) A developmental change in NMDA receptor-associated proteins at hippocampal synapses. J Neurosci 20:1260–1271. Medline

Sheng M, Cummings J, Roldan LA, Jan YN, Jan LY (1994) Changing subunit composition of heteromeric NMDA receptors during development of rat cortex. Nature 368:144–147. CrossRef Medline

Sloan HL, Good M, Dunnett SB (2006) Double dissociation between hippocampal and prefrontal lesions on an operant delayed matching task and a water maze reference memory task. Behav Brain Res 171:116–126. CrossRef Medline

Smith JW, Gastambide F, Gilmour G, Dix S, Foss J, Lloyd K, Malik N, Tricklebank M (2011) A comparison of the effects of ketamine and phencyclidine with other antagonists of the NMDA receptor in rodent assays of attention and working memory. Psychopharmacology (Berl) 217:255–269. CrossRef Medline

Sonntag WE, Bennett SA, Khan AS, Thornton PL, Xu X, Ingram RL, Brunso-Bechtold JK (2000) Age and insulin-like growth factor-1 modulate N-methyl-D-aspartate receptor subtype expression in rats. Brain Res Bull 51:331–338. CrossRef Medline

Sotres-Bayon F, Diaz-Mataix L, Bush DE, LeDoux JE (2009) Dissociable roles for the ventromedial prefrontal cortex and amygdala in fear extinction: NR2B contribution. Cereb Cortex 19:474–482. CrossRef Medline

Tovar KR, Westbrook GL (1999) The incorporation of NMDA receptors with a distinct subunit composition at nascent hippocampal synapses in vitro. J Neurosci 19:4180–4188. Medline

Townsend M, Yoshii A, Mishina M, Constantine-Paton M (2003) Developmental loss of miniature N-methyl-d-aspartate receptor currents in NR2A knockout mice. Proc Natl Acad Sci U S A 100:1340–1345. CrossRef Medline

Vicini S, Wang JF, Li JH, Zhu WJ, Wang YH, Luo JH, Wolfe BB, Grayson DR (1998) Functional and pharmacological differences between recombinant N-Methyl-d-aspartate receptors. J Neurophysiol 79:555–566. Medline

Walker DL, Davis M (2008) Amygdala infusions of an NR2B-selective or an NR2A-preferring NMDA receptor antagonist differentially influence fear conditioning and expression in the fear-potentiated startle test. Learn Mem 15:67–74. CrossRef Medline

Wang H, Stradtman GG 3rd, Wang XJ, Gao WJ (2008) A specialized NMDA receptor function in layer 5 recurrent microcircuitry of the adult rat prefrontal cortex. Proc Natl Acad Sci U S A 105:16791–16796. CrossRef Medline

Wang M, Yang Y, Wang CJ, Gamo NJ, Jin LE, Mazer JA, Morrison JH, Wang XJ, Arnsten AF (2013) NMDA receptors subserve persistent neuronal firing during working memory in dorsolateral prefrontal cortex. Neuron 77:736–749. CrossRef Medline

Wei H, Gong N, Huang JL, Fan H, Ma AN, Li XY, Wang YX, Pertovaara A (2013) Spinal D-amino acid oxidase contributes to mechanical pain hypersensitivity induced by sleep deprivation in the rat. Pharmacol Biochem Behav 111:30–36. CrossRef Medline

Zamzow DR, Elias V, Shumaker M, Larson C, Magnusson KR (2013) An increase in the association of GluN2B containing NMDA receptors with membrane scaffolding proteins was related to memory declines during aging. J Neurosci 33:12300–12305. CrossRef Medline

Zhang XH, Wu LJ, Gong B, Ren M, Li BM, Zhuo M (2008) Induction- and conditioning-protocol-dependent involvement of NR2B-containing NMDA receptors in synaptic potentiation and contextual fear memory in the hippocampal CA1 region of rats. Mol Brain 1:9. CrossRef Medline

Zhao X, Rosenke R, Kronemann D, Brim B, Das SR, Dunah AW, Magnusson KR (2009) The effects of aging on N-methyl-d-aspartate receptor subunits in the synaptic membrane and relationships to long-term spatial memory. Neuroscience 162:933–945. CrossRef Medline